Efficacy, safety and novel targets in cardiovascular disease : advanced applications in APOE*3-Leiden.CETP mice

Pouwer, M.G.


7

The APOE*3-Leiden heterozygous glucokinase knockout mouse as novel translational disease model for type 2 diabetes, dyslipidemia, and diabetic atherosclerosis

Marianne G. Pouwer*, Suvi E. Heinonen*, Margareta Behrendt, Anne-Christine Andréasson, Arianne van Koppen, Aswin L. Menke, Elsbet J. Pieterman, Anita M. van den Hoek, J. Wouter Jukema, Brendan Leighton, Ann-Cathrine Jönsson-Rylander, Hans M. G. Princen

*These authors contributed equally

J Diabetes Res. 2019 Feb 21;2019:9727952

Abstract

Objectives: There is a lack of predictive preclinical animal models combining atherosclerosis and type 2 diabetes. APOE*3-Leiden (E3L) mice are a well-established model for diet-induced hyperlipidemia and atherosclerosis, and glucokinase$^{+/-}$ (GK$^{+/-}$) mice are a translatable disease model for glucose control in type 2 diabetes. The respective mice respond similarly to lipid-lowering and antidiabetic drugs as humans. The objective of this study was to evaluate/characterize the APOE*3-Leiden.Glucokinase$^{+/-}$ (E3L.GK$^{+/-}$) mouse as a novel disease model to study the metabolic syndrome and diabetic complications.

Methods and results: Female E3L.GK$^{+/-}$, E3L, and GK$^{+/-}$ mice were fed fat- and cholesterol-containing diets for 37 weeks, and plasma parameters were measured throughout. Development of diabetic macro- and microvascular complications was evaluated. Cholesterol and triglyceride levels were significantly elevated in E3L and E3L.GK$^{+/-}$ mice compared to GK$^{+/-}$ mice, whereas fasting glucose was significantly increased in E3L.GK$^{+/-}$ and GK$^{+/-}$ mice compared to E3L. Atherosclerotic lesion size was increased 2.2-fold in E3L.GK$^{+/-}$ mice as compared to E3L ($p=0.037$), which was predicted by glucose exposure ($R^2=0.636$; $p=0.001$). E3L and E3L.GK$^{+/-}$ mice developed NASH with severe inflammation and fibrosis which, however, was not altered by introduction of the defective GK phenotype, whereas mild kidney pathology with tubular vacuolization was present in all three phenotypes.

Conclusions: We conclude that the E3L.GK$^{+/-}$ mouse is a promising novel diet-inducible disease model for investigation of the etiology and evaluation of drug treatment on diabetic atherosclerosis.

Introduction

The metabolic syndrome consists of a cluster of cardiovascular risk factors, including abdominal obesity, elevated blood pressure, elevated fasting plasma glucose, high serum triglycerides, and low high-density lipoprotein (HDL) levels, and drives the global epidemics of type 2 diabetes (T2D) and cardiovascular disease (CVD). Diabetes increases the CVD risk about twofold (1–3), which is the leading cause of death worldwide, and aggravates nonalcoholic steatohepatitis (NASH) (4) and diabetic nephropathy (5). These comorbidities emphasize the need for antidiabetic treatments that are effective against both T2D and associated cardiovascular complications.

Animal models can be used to learn more about the underlying pathology of diabetic complications and the effect of pharmacological interventions thereon, and a wide range of mouse models combining atherosclerosis and diabetes are described (6). Most available models are dyslipidemic mice, e.g., apoE$^{-/-}$ and LDLr$^{-/-}$ mice, with chemically (STZ) or genetically (ob/ob, db/db, and IRS2$^{-/-}$) induced diabetes (6). Although these models are widely used in biomedical research and drug development, they do not sufficiently reflect human disease. First, deficiency of the *Apoe* or *Ldlr* gene and STZ treatment result in extreme hyperlipidemia and hyperglycemia, respectively, and may result in overestimation of the contribution of hyperglycemia to diabetic complications. Besides, STZ treatment is difficult to control and creates a type 1 diabetic-like condition. Second, commonly used animal models of T2D (ob/ob and db/db mice) have a wide but unstable hyperglycemic range (7,8) and are monogenic models of obesity thereby inducing hyperglycemia, which weakens their translatable value as obesity is seldom caused by a monogenic mutation (7,9). Last, apoE$^{-/-}$ and LDLr$^{-/-}$ mice do not respond well to lipid-lowering drugs used in the clinic (10,11), making these models unsuitable in the development of novel therapeutic strategies against hyperlipidemia and vascular complications.

The objective of this study was to develop a translational mouse model for the metabolic syndrome and diabetic complications by combining diet-induced dyslipidemia and hyperglycemia, with plasma levels translatable to the human situation: the APOE*3-Leiden.Glucokinase$^{+/-}$ mouse (E3L.GK$^{+/-}$). We have generated the E3L.GK$^{+/-}$ mouse by cross-breeding dyslipidemic APOE*3-Leiden (E3L) mice with hyperglycemic heterozygous glucokinase knockout (GK$^{+/-}$) mice. The E3L mouse was initially developed as an animal model for mixed dyslipoproteinemia and was generated by the introduction of a DNA construct obtained from a patient with Familial Dysbetalipoproteinemia (FD) or type III hyperlipoproteinemia containing the human *APOE*3LEIDEN* and *APOC1* genes (12). Apoc1 is an inhibitor of lipoprotein lipase (LPL) and inhibits lipolysis of triglyceride-rich lipoproteins. The E*3-Leiden mutation results in a dysfunctional protein with reduced binding to the low-density lipoprotein receptor (LDLr) which leads to impaired clearance of triglyceride- and cholesterol-rich lipoproteins (chylomicron and VLDL remnants), thereby mimicking the slow clearance observed in humans, particularly in FD patients. E3L

mice are prone to develop hyperlipidemia and atherosclerosis upon feeding a Western-type diet containing saturated fat and cholesterol (13), and they respond similarly as humans do to lipid-modulating interventions that are being used in the clinic (e.g., statins, fibrates, niacin, and PCSK9 inhibitors) (11,14–22).

Glucokinase (GK) catalyzes the first and rate-limiting step in glycolysis, phosphorylation of glucose to glucose-6-phosphate, and acts as a "glucose sensor" in controlling glucose-stimulated insulin secretion (23). Loss of function mutations in the *GK* gene in man results in persistent hyperglycemia, referred to as maturity-onset diabetes of the young type 2 (MODY2) (24,25). Various transgenic animals with global or tissue-specific GK knockouts have been generated, each with specific characteristics with respect to metabolic control (26). In this study, we used the global heterozygous GK knockout mouse, which has reduced GK activity in both liver and pancreatic β-cells (26). $GK^{+/-}$ mice are moderately hyperglycemic when on chow, become diabetic on a high-fat diet (HFD) (26), and respond well to glucose-lowering therapeutic agents (e.g., metformin, sitagliptin, insulin, and exendin-4) (8,27).

Materials and methods

Animals and breeding

10–23-week old female E3L, $GK^{+/-}$, and E3L.$GK^{+/-}$ mice (n=6-10/sex/genotype) were used in the study. Both E3L and $GK^{+/-}$ mice are bred on a C57BL/6J background. Since homozygous E3L mice are not viable in utero, these mice are bred heterozygously by breeding E3L X C57BL/6J. $GK^{+/-}$ mice are bred heterozygously ($GK^{+/-}$ X C57BL/6J) as described previously (26), because the homozygous deletion of GK is postnatally lethal. E3L.$GK^{+/-}$ mice were generated by cross-breeding E3L mice with $GK^{+/-}$ mice, thereby generating 27 to 40% offspring of each genotype. Mice were crossed once and were not backcrossed. E3L mice are huApoE3Leiden-huApoC1 double transgenic mice, with both genes located on one genomic DNA construct (12), and therefore, the presence of the E3L phenotype was evaluated by genotyping for *APOC1*. The presence of the $GK^{+/-}$ phenotype was evaluated by qPCR as described previously (26). Females were used because E3L females are more responsive to dietary cholesterol and fat than males. E3L females have a higher VLDL production than males (28) resulting in higher plasma total cholesterol (TC) and triglyceride (TG) levels and development of atherosclerosis (12,29). All mice were housed under standard conditions with a 12 h light-dark cycle and had free access to food and water. Body weight was monitored regularly during the study. Animal experiments were approved by the Regional Animal Ethics Committee for Experimental Animals, Göteborg University. All *in vivo* activities were carried out conforming to the Swedish Animal Welfare Act and regulations SJVFS 2012: 26.

Experimental design and analyses

First, mice were fed a semisynthetic diet, containing saturated fat with 15% (w/w) cacao butter (Western-type diet (WTD); Hope Farms, Woerden, the Netherlands) and 0.15% cholesterol for 7 weeks to study the effect of a mildly lipid-elevating diet on plasma lipid and glucose levels. Subsequently, this diet was supplemented with 10% glucose in the drinking water in weeks 6–7 to investigate whether dietary glucose did modulate these plasma levels. During the following 30 weeks, mice were fed a WTD + 1.0% cholesterol to induce atherosclerosis (20) (**Figure 1**). EDTA blood samples were drawn after a 4-hour fast, and plasma parameters were evaluated at different time points throughout the study. The last blood sample was drawn at week 36, and all animals were sacrificed by CO_2 inhalation at week 37. Plasma TC, TG, glucose, and insulin were measured throughout the study, and HbA1c was measured at week 36. TC and glucose exposure were calculated by adding up for all intervals the products of the mean cholesterol or glucose level during that interval times the duration of that interval and expressed as mmol/L*weeks. Lipoprotein profiles, alanine transaminase (ALT), and aspartate transaminase (AST) were measured in group wise-pooled unfasted sacrifice plasma. Urinary albumin:creatinine levels were measured in spot urine collected in week 36. Hepatic lipid content was analyzed in homogenized, snap-frozen liver samples as described previously (30). Heart and aorta, liver, and kidneys were collected for histopathological analysis of atherosclerosis, NAFLD/NASH and liver fibrosis, and diabetic nephropathy.

Biochemical analyses

Plasma TC and TG were determined throughout the study using enzymatic colorimetric methods (TC: kit no. A11A01634, Horiba ABX, France and TG: kit no. 12146029, Roche Diagnostics GmbH, Germany) according to the manufacturer's protocols and TC exposure was calculated. HDL-C was measured after precipitation of apoB-containing particles (31). The distribution of cholesterol over plasma lipoproteins was determined in group wise-pooled unfasted sacrifice plasma by fast protein liquid chromatography (FPLC) (32). Blood glucose and HbA1C levels were measured in one drop of blood obtained from the

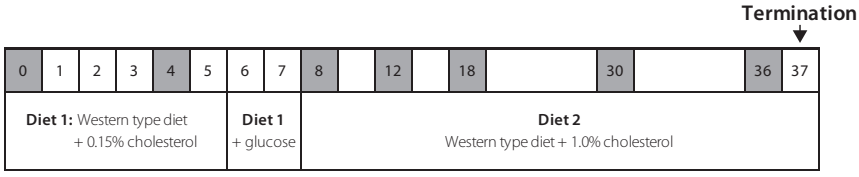

Figure 1 Study design. Female E3L.GK$^{+/-}$, E3L, and GK$^{+/-}$ mice were fed different diets throughout the study. Blood samples were drawn at weeks 0, 4, 8, 12, 18, 30, and 36 as depicted in grey. All mice were sacrificed at week 37. +glucose: 10% glucose drinking water.

tail in awake mice, using Accu-Chek (Roche, REF 05599415370) and HbA1C Now+ (Bayer, REF81611409-3038), respectively, and total glucose exposure was then calculated. Plasma insulin levels were measured with a radioimmunoassay (SRI-13K, Millipore Corporation, USA) on a 1470 Automatic Gamma Counter (PerkinElmer, USA). Plasma ALT and AST were determined using a spectrophotometric assay (Boehringer Reflotron system) in group wise-pooled samples. Urinary albumin and creatinine levels were determined using the mouse albumin ELISA kit (ALPCO, Salem, USA) and the creatinine kit (Exocell, Philadelphia, USA). All assays were performed according to manufacturer's instruction. Hepatic lipid content was analyzed in homogenized, snap-frozen liver samples and analyzed with TINA2.09 software (Raytest Isotopen Meβgeräte, Straubenhardt, Germany).

Histological assessment of atherosclerosis

Hearts were fixed in formalin, embedded in paraffin and sectioned perpendicular to the axis of the aorta. Serial cross sections (5 µm thick with intervals of 50 µm) were stained with hematoxylin-phloxine-saffron (HPS) for histological analysis. The average total lesion area per cross-section was then calculated (31,33). For determination of lesion severity the lesions were classified into five categories according to the American Heart Association classification (34): 0) no lesion, I) early fatty streak, II) regular fatty streak, III) mild plaque, IV) moderate plaque, and V) severe plaque. Lesion composition was determined for the type III-V lesions as a percentage of lesion area after immunostaining with anti-human alpha-actin (1:400; PROGEN Biotechnik GmbH, Germany. Cat#:61001) for smooth muscle cells (SMC), anti-mouse Mac-3 (1:50; BD Pharmingen, the Netherlands. Cat#: 550292) for macrophages and Sirius Red staining for collagen. Necrotic area and cholesterol clefts were measured after HPS staining. Lesion stability index was calculated as described previously (31,33). In each segment used for lesion quantification, the number of monocytes adhering to the endothelium was counted after immunostaining with AIA 31240 antibody (1:1000; Accurate Chemical and Scientific, New York, New York, USA. Cat#: J1857) (31). Lesion areas were measured using Cell D imaging software (Olympus Soft Imaging Solutions).

Histological assessment of liver steatosis and fibrosis

Liver samples (lobus sinister medialis hepatis) were collected from non-fasted mice, fixed in formalin and paraffin embedded, and sections (3 µm) were stained with hematoxylin and eosin (HE) and Sirius Red. Hepatic steatosis was scored blinded by a board-certified pathologist in HE-stained cross-sections using an adapted grading system of human NASH (35,36). Hepatic fibrosis was identified using Sirius Red stained slides and evaluated using an adapted grading system of human NASH (35,37), in which the presence of pathological collagen staining was scored as either absent (0), observed within perisinusoidal/perivenular or periportal area (1), within both perisinusoidal and periportal areas (2), bridging fibrosis (3) or cirrhosis (4). In addition, liver fibrosis (expressed as the

percentage of the total liver tissue area) was quantified automatically using ImageJ software (version 1.48, NIH, Bethesda, MD, USA) (38).

Histological assessment of diabetic nephropathy

Left kidneys were fixed in formalin, embedded in paraffin and sections (3 µm) were stained with HE, Masson's trichrome (MTC), periodic acid–Schiff (PAS) and immunohistochemically for nephrin. Nephrin was stained using a Ventana Discovery with an antibody raised in guinea pig (ab6698, Abcam) diluted 1:1000, Link Rb@GP (Abcam) diluted 1:500, followed by OmniMap@Rb HRP (ROCHE) and ChromoMap DAB-kit (Roche) was used to detect the positive reaction. Sections were finally counterstained with HE (Roche). An overall score based on the combination of all evaluated parameters was determined blinded by a board-certified pathologist where 0 indicates no change in morphology and 5 indicates severe morphological changes. Vacuolized tubuli were scored as 0 indicating that no vacuolized tubuli are present, 1 indicating small and few vacuoles and 2 indicating large and many vacuoles. Sections stained with HE were evaluated for the presence of renal damage focusing on glomerular damage, including mesangial matrix expansion, and tubule-interstitial damage, including interstitial inflammation, fibrosis and tubular abnormalities, as central causes for loss of kidney function. MTC was used for detection of fibrosis, PAS for scoring of matrix expansion and protein deposition in the tubuli, and nephrin for confirmation of matrix expansion and deletion of nephrin.

Statistical analysis

The E3L.GK$^{+/-}$ phenotype was compared to E3L and GK$^{+/-}$, and significance of differences was calculated parametrically using a one-way ANOVA with Dunnett's post hoc test. Differences in plasma parameters between the different time points were calculated for each genotype using a one-way ANOVA with a Bonferroni post hoc test. Significance of differences between the E3L.GK$^{+/-}$ and E3L mice in atherosclerotic lesion number, severity, and composition was calculated using an independent sample *t*-test. A multiple regression analysis was performed to predict the effect of variables on lesion size, and linear regression was used to assess correlations between variables. SPSS 22.0 for Windows was used for statistical analysis. Values are presented as means ± SD. All reported p-values < 0.05 were considered statistically significant.

Results

Safety aspects

No clinical signs of deviant behavior were noted in any of the phenotypes. From week 0 to 36, all three phenotypes gained 5 ± 2 gram body weight (**Table 1**). Plasma pooled per group showed lower AST and ALT values as markers of hepatocellular damage in GK$^{+/-}$ mice when compared to E3L.GK$^{+/-}$ and E3L (**Table 1**). One mouse was terminated during the study based on human end-point criteria.

Table 1 Biochemical parameters in E3L. GK$^{+/-}$, E3L and GK$^{+/-}$ mice

	E3L.GK$^{+/-}$	E3L	GK$^{+/-}$
Weight gain (g)	5 ± 2	5 ± 2	5 ± 2
Weight gain (% of body weight at t=0)	23 ± 6	24 ± 6	24 ± 11
Liver weight (g)	1.9 ± 0.3†	2.0 ± 0.4	1.4 ± 0.3
Liver weight (% of body weight at t=36)	8 ± 1††	8 ± 2	6 ± 1
Cholesterol (mmol/L)	14 ± 3†††	12 ± 3	2 ± 1
Triglycerides (mmol/L)	2.0 ± 0.8†††	1.7 ± 0.4	0.5 ± 0.1
Glucose (mmol/L)	10 ± 1***	8 ± 1	12 ± 2
Insulin (ng/mL)	0.4 ± 0.3	0.1 ± 0.1	0.2 ± 0.1
HbA1c (%)	5.1 ± 0.6**	4.3 ± 0.2	5.4 ± 0.4
ALT (U/L)	272	199	30
AST (U/L)	660	402	125
Urinary albumin:creatinin	19 ± 11	16 ± 2	31 ± 34

All depicted parameters are measured at week 36, except for liver weight (week 37). ** P<0.01, *** P<0.001 when compared to E3L; †P<0.05, †† P<0.01, ††† P<0.001 when compared to GK+/- . Data are presented as means ± SD (n = 8-10 per group and insulin n=4-8 per group).

Plasma parameters for metabolic disease and response to diets

E3L.GK$^{+/-}$ mice are hyperlipidemic and hyperglycemic

Plasma TC and TG levels in E3L.GK$^{+/-}$ mice were similar to E3L mice and increased by 540% (TC) and 450% (TG) when compared to GK$^{+/-}$ mice (**Figure 2A and B**), resulting in a significantly increased cholesterol exposure (mmol/L*weeks) (+316%, p<0.001) (**Figure 2D**). Cholesterol in the E3L and E3L.GK$^{+/-}$ mice was mainly contained in VLDL and LDL, and in GK$^{+/-}$ in HDL (**Figure 2C**). Glucose levels were significantly elevated at all time points except at t=4 weeks when compared to E3L mice (**Figure 2E**). Total glucose exposure (mmol/L*weeks) was 429 ± 60, 299 ± 14 and 492 ± 52 mmol/L for E3L.GK$^{+/-}$, E3L and GK$^{+/-}$, respectively, and significantly increased in E3L.GK$^{+/-}$ when compared to E3L mice (+40%,

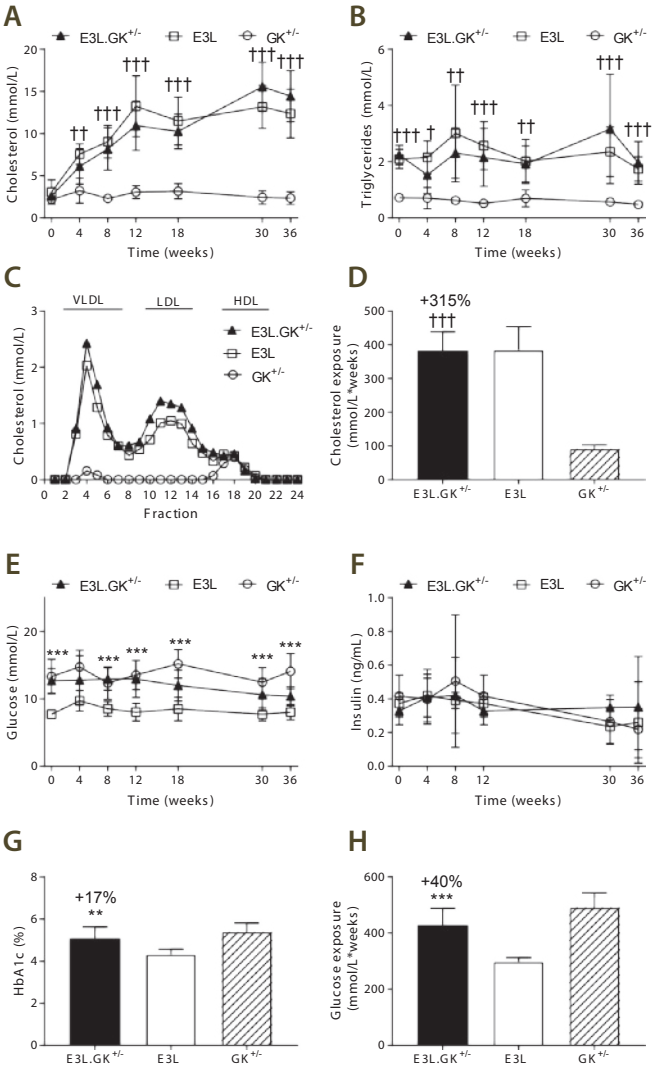

Figure 2 E3L.GK+/– mice have comparable lipid levels and higher glucose levels as E3L mice. Plasma cholesterol (A) and triglycerides (B) were measured throughout the study. Lipoprotein profiles were assessed by FPLC lipoprotein separation in group wise-pooled unfasted sacrifice plasma (C). Cholesterol exposure over time was calculated as mmol/L*weeks (D). Plasma glucose (E) and insulin (F) were measured throughout, HbA1c (%) was measured at week 36 (G), and glucose exposure was calculated as mmol/L*weeks (H). Data are presented as means ± SD (n=8-10 per group and for insulin n=4-8 per group). E3L.GK+/– compared to E3L. *p<0.05, **p<0.01, and ***p<0.001; E3L.GK+/– compared to GK+/–: †p<0.05, ††<0.01, and ††† p<0.001. Abbreviations: FPLC, fast protein liquid chromatography; HbA1c, hemoglobine A1c.

p<0.001) (**Figure 2H**). Insulin levels did not differ between the strains (**Figure 2F**). HbA1c was increased by 17% when compared to E3L mice (p=0.005) (**Figure 2G**). In conclusion, these data show that E3L.GK$^{+/-}$ combine both adverse phenotypes with increased lipid levels as in E3L mice and mildly elevated glucose levels as of GK$^{+/-}$ mice.

Plasma cholesterol levels are modulated by the diet in E3L.GK$^{+/-}$ and E3L mice

Different diets were used in this study to evaluate the response of the mouse model to dietary interventions. Plasma TC, but not TG, increased in both E3L.GK$^{+/-}$ and E3L mice when switched from a chow diet (t=0 weeks) to a WTD with 0.15% cholesterol added (+143%, p=0.038; +173%, p=0.001), whereas plasma lipid levels were not affected in GK$^{+/-}$ mice (**Table 2**). Plasma glucose and insulin levels were not affected by the WTD with 0.15% cholesterol added, except for glucose which increased in E3L mice (+26%, p=0.010). Adding 10% glucose to the drinking water further increased plasma TC levels: when compared to t=0 weeks (chow) TC levels increased by 215% in E3L.GK$^{+/-}$ mice (p=0.001) and by 224% in E3L mice (p<0.001). However, this increase was not significant when compared to t=4 (WTD with 0.15% cholesterol) (**Table 2** Increasing the amount of cholesterol in the diet to 1.0%, further increased plasma TC levels in E3L.GK$^{+/-}$ and E3L mice when compared to t=0 and when compared to t=8 (+89%, p<0.001; +43%, p=0.013). Insulin levels dropped in E3L mice at t=36 weeks when compared to t=0 weeks (-60%, p=0.020) and t=8 weeks (-66%, p=0.010), whereas this effect was less pronounced in GK$^{+/-}$ mice (-41%, p=0.081 compared to t=8 weeks), and absent in E3L.GK$^{+/-}$ mice. Interestingly, plasma glucose levels in E3L.GK$^{+/-}$ and GK$^{+/-}$ mice were not modulated by glucose in the drinking water, indicating that despite reduced glucokinase activity (26) the mice maintain their glucose homeostasis at increased glucose supply. Altogether, these data show that plasma lipids can be modulated in the E3L.GK$^{+/-}$ mouse model, as in E3L mice, whereas the elevated glucose levels on chow are not further increased by these dietary interventions.

Diabetic macro- and microvascular complications in E3L.GK$^{+/-}$ mice

Atherosclerotic lesion size and severity are aggravated in E3L.GK$^{+/-}$ mice

One of the most important diabetic complications is increased risk for CVD (1–3) and therefore, we assessed atherosclerotic lesion size, lesion severity and plaque phenotype, as marker of vulnerability to rupture, in the aortic root. E3L mice developed 0.4 ± 0.5 mild (I-II), 3.6 ± 2.3 moderate (III) and 1.6 ± 1.8 severe (IV-V) lesions per cross-section. The number of severe lesions was significantly increased in E3L.GK$^{+/-}$ mice (2.8-fold; p=0.038) (**Figure 3A**). When lesion severity was depicted as the percentage of total plaque area that consisted of mild or severe lesions, there was no difference between E3L and E3L.GK$^{+/-}$ mice (**Figure 3B**). However, the total atherosclerotic lesion size was significantly increased by 2.2-fold in the E3L.GK$^{+/-}$ mice (68 ± 42 *1000 μm^2) as compared to E3L (32 ± 29 *1000 μm^2) (p=0.037) (**Figure 3C**). There were no lesions visible in the GK$^{+/-}$ mice (**Figure 3C**). The plaque composition was analyzed in the type III-V lesions, as illustrated by representative images

Table 2 Plasma cholesterol levels are modulated by the diet in E3L.GK$^{+/-}$ and E3L mice

Diet at time of plasma sample		Chow	WTD + 0.15% cholesterol		WTD + 0.15% cholesterol and 10% glucose drinking water			WTD + 1.0% cholesterol		
Time (weeks)		*0*	*4*		*8*			*36*		
			mmol/L[*1]	relative to t=0 (%)	mmol/L[*1]	relative to t=0 (%)	relative to t=4 (%)	mmol/L[*1]	relative to t=0 (%)	relative to t=8 (%)
TC	E3L.GK$^{+/-}$	2.6 ± 0.3	6.1 ± 2.1*	143	8.2 ± 2.5**	215	64	14.4 ± 3.0***/†††	463	89
	E3L	3.1 ± 1.5	7.6 ± 1.2**	173	9.0 ± 1.9***	224	20	12.4 ± 2.9***/†	353	43
	GK$^{+/-}$	2.2 ± 0.4	3.2 ± 1.5	60	2.3 ± 0.3	9	-20	2.3 ± 0.8	11	4
TG	E3L.GK$^{+/-}$	2.2 ± 0.3	1.5 ± 0.7	-30	2.3 ± 0.9	3	95	2.0 ± 0.8	-14	-5
	E3L	2.1 ± 0.3	2.2 ± 0.6	5	3.0 ± 1.7	45	45	1.7 ± 0.4	-15	-28
	GK$^{+/-}$	0.7 ± 0.0	0.7 ± 0.4	-2	0.6 ± 0.1	-14	1	0.5 ± 0.1	-33	-19
Glucose	E3L.GK$^{+/-}$	12.7 ± 1.8	12.8 ± 3.6	1	13.0 ± 1.7	4	7	10.4 ± 1.4	-19	-17
	E3L	7.7 ± 0.7	9.7 ± 1.5*	26	8.5 ± 1.1	11	-10	8.0 ± 1.2	5	-4
	GK$^{+/-}$	13.3 ± 2.6	14.7 ± 2.5	14	12.4 ± 2.4	-6	-14	14.1 ± 2.6	9	17
Insulin	E3L.GK$^{+/-}$	0.3 ± 0.1	0.4 ± 0.1	30	0.4 ± 0.2	43	8	0.4 ± 0.3	-13	9
	E3L	0.4 ± 0.1	0.4 ± 0.2	15	0.4 ± 0.0	7	3	0.1 ± 0.1*/†	-60	-66
	GK$^{+/-}$	0.4 ± 0.1	0.4 ± 0.1	3	0.5 ± 0.4	32	24	0.2 ± 0.1	-42	-41

The response of plasma lipids, glucose and insulin to the different diets was evaluated. Data are presented as means ± SD (n=8-10 per group and insulin n=4-8 per group). * P<0.05, ** P<0.01, *** P<0.001 when compared to T = 0 weeks; †P<0.05, ††† P<0.001 when compared to previous time point. [*1] Insulin (ng/mL). Abbreviations: WTD, western type diet.

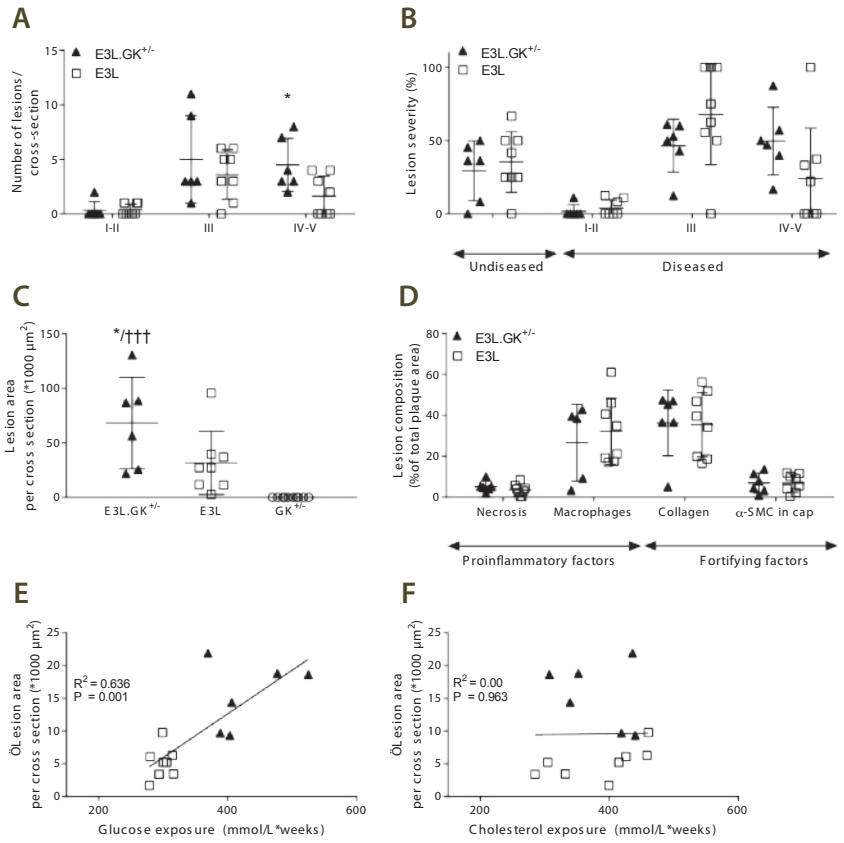

Figure 3 Atherosclerotic lesion size and severity are aggravated in E3L.GK$^{+/-}$ mice which is correlated to glucose exposure. The number of lesions (A), lesion severity classified as mild (type I-II lesions), moderate (type III) and severe (type IV and V) lesions (B), and atherosclerotic lesion size per cross-section (C). Necrotic and macrophage content as pro-inflammatory factors, and αSMCs and collagen as fortifying factors, were determined in type III-V lesions and expressed as percentage of total plaque area (D). Linear regression analyses were performed on the square root of the lesion area plotted against glucose exposure (E) or cholesterol exposure (F). Data are presented as means ± SD (n = 6-8 per group).*P<0.05 when compared to E3L; ††† P<0.001 when compared to GK$^{+/-}$.

in **Figure 4**. There were no significant differences between E3L.GK$^{+/-}$ and E3L mice in plaque composition (**Figure 3D**), plaque stability index or monocyte adherence to the endothelium (data not shown). Collectively, these data show that atherosclerotic lesion size is aggravated in E3L.GK$^{+/-}$ as compared to E3L mice without affecting plaque composition and monocyte adherence.

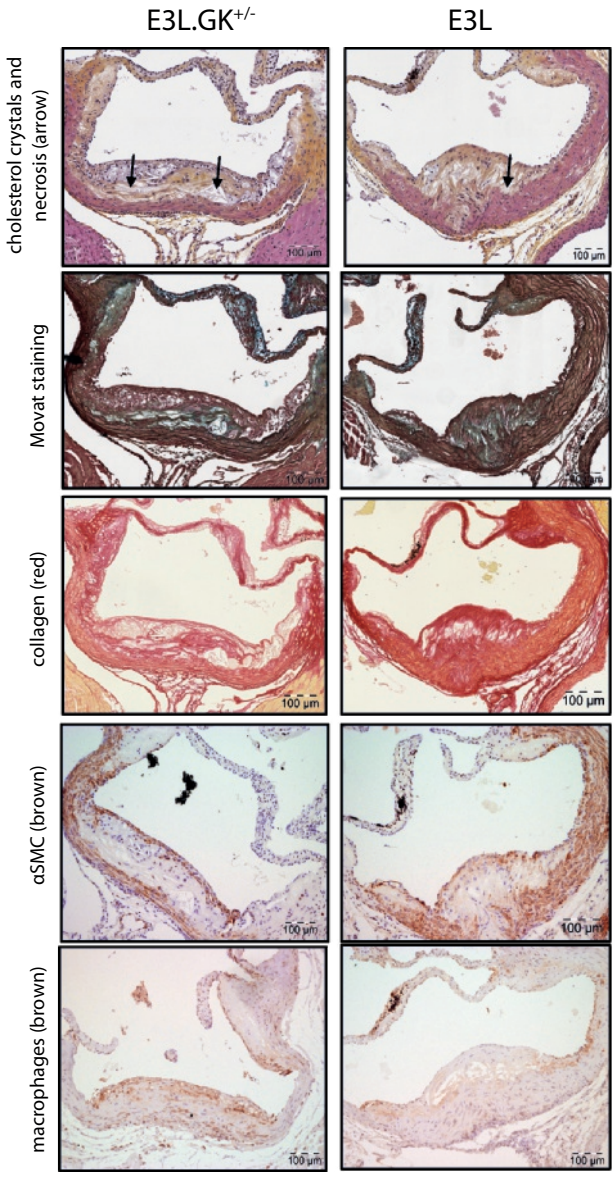

Figure 4 Plaque composition in a severe plaque of a E3L and E3L.GK$^{+/-}$ mouse. Representative images of HPS staining, Movat staining, Sirius red staining for collagen, immunostaining with α-actin for SMCs and immunostaining with Mac-3 for macrophages. The arrows depict necrotic areas, including cholesterol clefts. Abbreviations: HPS, hematoxylin-phloxine-saffron; SMCs, smooth muscle cells.

Elevated plasma glucose levels contribute to the increased development of atherosclerosis in E3L.GK$^{+/-}$ mice

To explore the contribution of the elevated plasma glucose levels to the increased lesion size, a multiple regression analysis was performed with cholesterol and glucose exposure as covariates after square root transformation of the lesion area. Lesion size was predicted only by glucose exposure ($p<0.001$). In addition, univariate regression analysis showed a clear association of lesion size with glucose exposure ($R^2=0.636$, $p=0.001$) (**Figure 3E**) but not with cholesterol exposure (**Figure 3F**), pointing towards an important role for glucose in the accelerated atherosclerosis development in E3L.GK$^{+/-}$ mice.

The GK$^{+/-}$ phenotype does not aggravate hepatic steatosis, inflammation or fibrosis

NAFLD/NASH is strongly associated with the metabolic syndrome and type 2 diabetes (39,40). To assess whether the GK$^{+/-}$ phenotype worsens the development of NASH, liver sections were examined for hepatic steatosis, inflammation and fibrosis, and liver lipid content was measured. Hepatic macrosteatosis did not differ between the phenotypes (**Figure 5A**), whereas hepatic microsteatosis was significantly elevated by 2.7-fold ($p=0.003$) in E3L.GK$^{+/-}$ mice when compared to GK$^{+/-}$ (**Figure 5B**), and both E3L.GK$^{+/-}$ and E3L had severe liver inflammation which was 6.8-fold increased ($p<0.001$) in E3L.GK$^{+/-}$ relative to GK$^{+/-}$ (**Figure 5C**). Furthermore, mean fibrosis stage in E3L.GK$^{+/-}$ was significantly elevated when compared to GK$^{+/-}$ (2.3-fold, $p<0.001$) (**Figure 5D**), as well as the percentage Sirius red positive area of total liver area (6.1-fold, $p=0.011$) (**Figure 5E**). Liver lipids did not differ between the phenotypes (**Figure 5F-H**). Representative images are shown (**Figure 5I-N**). Collectively, these data show that E3L and E3L.GK$^{+/-}$ mice, but not GK$^{+/-}$, develop NASH with severe inflammation and fibrosis, which is not worsened by increased glucose levels. This indicates a dominant role for the combination of the E3L phenotype and dietary cholesterol in the progression of NASH and liver fibrosis.

Mild kidney pathology is present in all three phenotypes

Diabetic nephropathy is becoming an increasingly important cause of morbidity and mortality worldwide and is related to the increasing prevalence of type 2 diabetes. Therefore, kidneys were analyzed for the presence of renal damage focusing on glomerular damage, including mesangial matrix expansion, and tubulo-interstitial damage, including interstitial inflammation, fibrosis and tubular abnormalities, as central causes for loss of kidney function. Nephrin staining was performed to study renal filtration barrier function. There were no differences in inflammation, fibrosis (data not shown), mesangial matrix expansion (**Figure 6A**) or nephrin score (**Figure 6B**) between the phenotypes. Abnormal tubular structures were observed in all three phenotypes but were most pronounced in GK$^{+/-}$ mice, wherein the tubuli showed vacuolization (**Figure 6C**). The pathological changes did not affect permeability in the glomerulus, as measured by the urinary albumin:creatinine ratio (**Table 1**). Altogether, we can conclude that mild pathological changes are present, which are not aggravated in E3L.GK$^{+/-}$ mice.

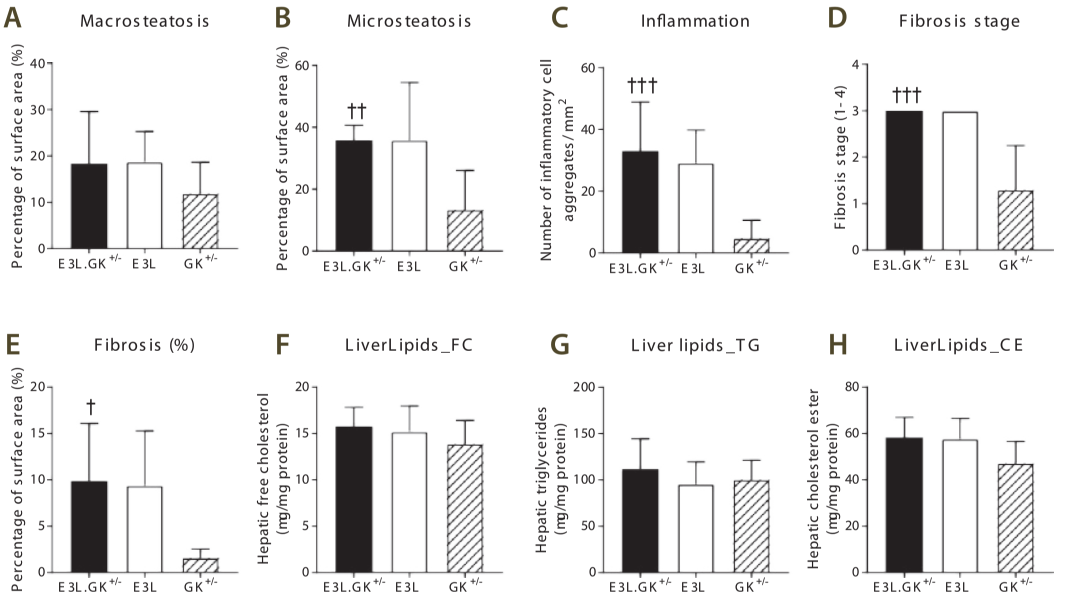

Figure 5 The GK phenotype does not aggravate hepatic steatosis, inflammation or fibrosis in E3L mice. Macrovesicular steatosis (A) and microvesicular steatosis (B) as percentage of total liver area was determined. The number of inflammatory cell aggregates were counted per mm^2 (C). Fibrosis grade (1-4) was scored (D) and percentage of area positive for Sirius Red was measured in ImageJ (E). Intrahepatic free cholesterol (F), intrahepatic triglycerides (G) and intrahepatic cholesterol esters (H) were analyzed by HPTLC. Representative images of HE (I-K) and Sirius Red (L-N) staining at a 5x magnification. Data are presented as means ± SD (n = 6-10 per group). † P<0.05, †† P<0.01, ††† P<0.001 when compared to $GK^{+/-}$. Abbreviations: HPTLC, high-performance thin-layer chromatography; HE, hematoxylin-eosin.

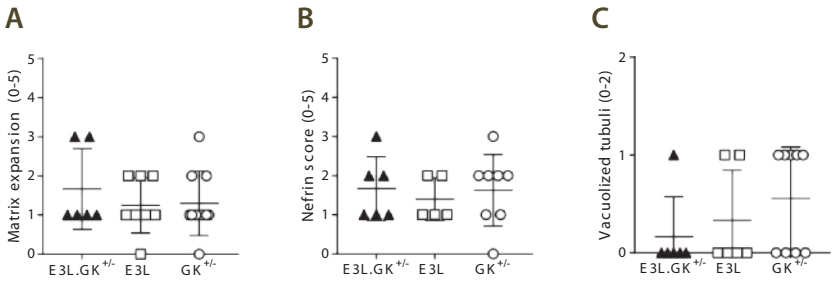

Figure 6 Mild matrix expansion and vacuolized tubuli in all phenotypes. Presence of matrix expansion (A), nephrin score (B) and vacuolized tubuli (C) was scored in a range of 0-5. Data are presented as means ± SD (n = 7-10 per group). .

Discussion

In the present study, we evaluated the E3L.GK$^{+/-}$ mouse as an animal model for diet-induced hyperlipidemia and hyperglycemia and the pathological consequences thereof. We showed that plasma lipids can be titrated to desired and for humans relevant levels by adding cholesterol and fat to the diet, and that these levels remain stable for a long period (up to 37 weeks). In addition, E3L.GK$^{+/-}$ mice were mildly hyperglycemic and developed more atherosclerosis than E3L mice, which was related to the higher glucose levels in the E3L.GK$^{+/-}$ mice. E3L and E3L.GK$^{+/-}$ mice both developed hepatic steatosis with severe inflammation and fibrosis, which, however, was not altered by introduction of the defective GK phenotype, whereas only mild kidney pathology with tubular vacuolization was present in all three phenotypes.

Translatability of animal models is essential when investigating the pathogenesis of diabetic complications and evaluating drug treatment thereon. Plasma cholesterol and glucose levels in the diet-induced E3L.GK$^{+/-}$ mouse model were similar to levels in patients with increased cardiovascular risk (2,41). Partial deletion of the *Gk* gene in the E3L mice did not affect the response of plasma lipids to dietary modulation, and in both E3L.GK$^{+/-}$ and E3L mice plasma cholesterol levels raised similarly upon feeding a WTD with increasing amounts of cholesterol. Interestingly, glucose and insulin levels were not affected by the diet, but remained stable representing mild hyperglycemia in E3L.GK$^{+/-}$ and GK$^{+/-}$ mice (10.4 ± 1.4 mmol/L and 14.1 ± 2.6 mmol/L at end-point, respectively). In contrast, glucose levels in male GK$^{+/-}$ mice increase over time on a high-fat diet with plasma levels reaching 18.9 ± 1.0 mmol/L and impaired glucose tolerance (8,26). This gender difference may be explained by the C57BL/6J background of the E3L and GK$^{+/-}$ transgenic mice. Upon a high-fat diet, insulin and glucose levels increase over time in C57BL/6J males, consistent

with insulin resistance and glucose intolerance, whereas C57BL/6J females have normal serum insulin concentrations and glucose levels remain constant (42). Estrogens affect different metabolic pathways in the glucose hemostasis (43), thereby protecting against the risk of developing type 2 diabetes in both pre-menopausal women (44) and mice (43).

We observed a markedly increased atherosclerotic lesion size in E3L.GK$^{+/-}$ as compared to E3L mice which was highly significantly correlated with glucose exposure (R^2=0.636, p=0.001), suggesting a pro-atherogenic role of glucose in the development of atherosclerosis. Indeed, it is known that prolonged exposure to hyperglycemia negatively affects the endothelium, vascular smooth muscle cells and macrophages, and it increases thrombosis while impairing fibrinolysis, leading to formation of atherosclerotic plaques (45). This may explain the association of diabetes type 2/hyperglycemia with cardiovascular disease as found in both humans (1,2,45,46) and hyperglycemic mice (6), including E3L.GK$^{+/-}$ mice.

In the present study, both the hyperglycemic GK$^{+/-}$ mice as well as the hyperlipidemic E3L and E3L.GK$^{+/-}$ mice developed hepatic steatosis, in line with the pathogenesis of NAFLD wherein both metabolic overload and hyperlipidemia contribute to the accumulation of triglycerides and cholesterol in the liver. Interestingly, E3L and E3L.GK$^{+/-}$, but not GK$^{+/-}$ mice, developed extensive inflammation and hepatic fibrosis, pointing towards a role for cholesterol in the transition of NAFLD to NASH. Consistent with this view, when cholesterol is supplied to HFD diet, E3L mice develop NASH and liver fibrosis as well (47), and E3L and E3L.CETP mice have been shown to be established diet-induced NASH and liver fibrosis models (47,48). In a previous study with E3L mice, an increased amount of hepatic cholesterol crystals was found and intrahepatic free cholesterol levels were positively correlated with the number of inflammatory aggregates and the expression of hepatic pro-inflammatory and pro-fibrotic genes (49). Similarly, it has been shown that accumulation of free cholesterol leading to the formation of cholesterol crystals in hepatocyte lipid droplets may trigger the progression of simple steatosis to NASH both in patients and in mice (50). Since no additional effects of glucose were observed on hepatic inflammation or fibrosis in E3L.GK$^{+/-}$ mice, we suggest that hyperlipidemia rather than hyperglycemia is an initiator of hepatic inflammation and fibrosis.

Chronic kidney disease is a largely irreversible disease characterized by tubulointerstitial inflammation, fibrosis, and glomerulosclerosis. The present study describes only mild kidney pathology without microalbuminuria in all three phenotypes. In addition to risk factors investigated in this study (hyperglycemia and dyslipidemia), hypertension plays a central role in renal injury through increasing renal tubular reabsorption and causing a hypertensive shift of renal-pressure natriuresis (5). Studies on nephropathic patients showed that decreased blood pressure reduced the incidence of renal events and improved kidney function (51,52). In the present study blood pressure was not measured. However, it is known that E3L mice do not develop hypertension upon a WTD, but do respond to anti-hypertensive treatment (15,17), and although there are no reports in GK$^{+/-}$ mice, GK deficiency in humans does not aggravate blood pressure (25).

Previously, the GK$^{+/-}$ApoE$^{-/-}$ mouse model has been developed as model combining hyperlipidemia and hyperglycemia, which had impaired glucose tolerance and a minimal increase of atherosclerosis relative to ApoE$^{-/-}$ mice (53). A disadvantage of this model is the ApoE$^{-/-}$ background. ApoE$^{-/-}$ mice are, like LDLR$^{-/-}$ mice, a severe model for hyperlipidemia, and due to the absence of a functional apoE-LDLR-mediated clearance pathway these mice do not respond well to lipid-lowering drugs (e.g. statins (10), PCSK9 inhibitors (11)) and therefore cannot be used for the evaluation of combination treatment. In contrast, E3L mice are very suited to study lipoprotein metabolism and lipid modulation (10,54).

In **Figure 7** we give an overview of all registered cholesterol- and glucose-lowering drugs that have been evaluated in E3L and GK$^{+/-}$ mice, respectively. E3L mice respond similarly as humans do to lipid lowering agents, including statins, fibrates, niacin and PCSK9-inhibitors (11,14–22), whereas glucose levels are successfully reduced in GK$^{+/-}$ mice by standard therapeutic agents as insulin, metformin, exendin-4 and GKAs at doses corresponding to therapeutic drug levels in man (8,27). Although these interventions have not been assessed in E3L.GK$^{+/-}$ mice yet, we carefully speculate about the effects and discuss how the model can be of value for future research. As E3L.GK$^{+/-}$ mice have similar lipid and glucose levels as their parent models, and respond in a similar way to dietary modulations, we propose that both lipid and glucose lowering agents will be effective in the combined model. Also, we propose that E3L.GK$^{+/-}$ mice can be used to examine interactions between glucose and lipid metabolism, e.g. how statin treatment increases the risk of diabetes incidence (55). Last, atherosclerosis development and CV safety can be evaluated in the E3L.GK$^{+/-}$ model, which is especially interesting regarding the currently unknown mechanisms by which glucose-lowering agents (e.g. empagliflozin, liraglutide, semaglutide) improve CV outcome (56–58).

Altogether, we conclude that the E3L.GK$^{+/-}$ mouse is a promising translatable diet-inducible model, combining dyslipidemia and hyperglycemia with human-like plasma cholesterol and glucose levels and aggravated atherosclerosis, to study the etiology of diabetic atherosclerosis and for the evaluation of lipid-lowering and anti-diabetic drugs and their combination thereon.

Acknowledgements

The authors thank Erik Offerman (TNO) and Marlieke Geerts (Leiden University Medical Centre, Leiden, the Netherlands) for their excellent technical assistance.

Disclosures

JWJ received research grants from and was speaker on (CME-accredited) meetings sponsored by Amgen, Astellas, Astra-Zeneca, Daiichi Sankyo, Lilly, Merck-Schering-Plough, Pfizer, Roche, Sanofi-Aventis, the Netherlands Heart Foundation, the Interuniversity Cardiology Institute of the Netherlands, and the European Community Framework KP7 Program. MB, ACA and ACJR are employees of AstraZeneca and SHE and BL were employees

of AstraZeneca during the execution of the study. MGP, AvK, ALM, EJP, AMvdH and HMGP have nothing to disclose.

Funding

This work was supported in part by AstraZeneca, Mölndal, Sweden, the TNO research program "Preventive Health Technologies" and the European Union Seventh Framework Programme (FP7/2007-2013) grant nr. 602936 (CarTarDis project).

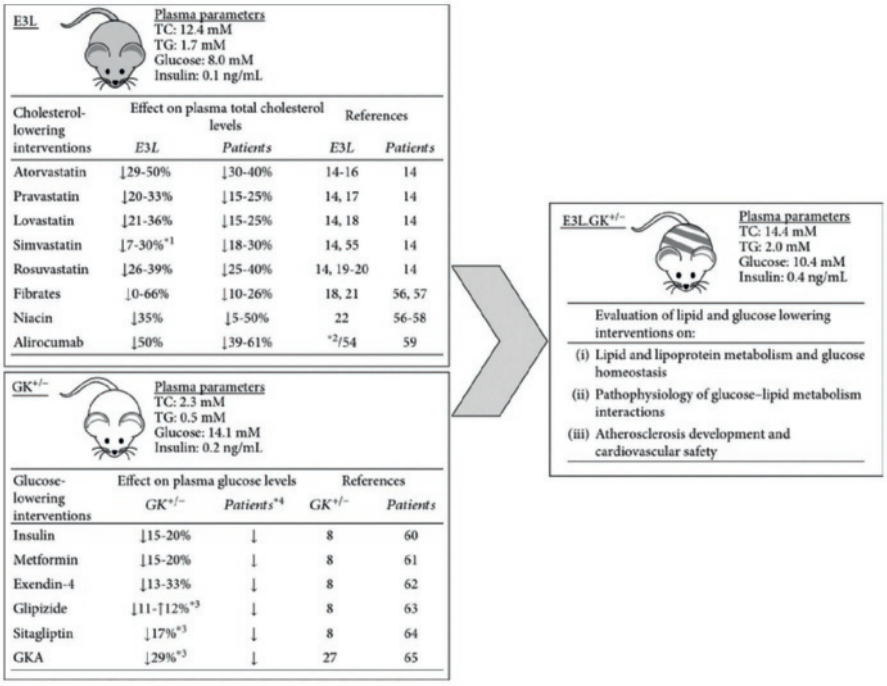

Figure 7 Overview of intervention studies with cholesterol- and glucose-lowering drugs performed in the E3L and GK+/- mouse models. The effects of cholesterol-lowering interventions on plasma TC levels were evaluated in E3L mice in long-term (5-28 weeks) exposure studies. The effects of glucose-lowering interventions on free-feeding blood glucose profiles were evaluated in GK+/- mice after single or repeated*3 dosing. In all studies, mice where fed a high fat or high fat/cholesterol containing diet. Data are extrapolated from published studies (see references). The depicted plasma parameters were measured at end-point in the present study. *1: Data shown of both APOE*3-Leiden and APOE*3-Leiden.CETP mice. *2: Unpublished. See reference 58 for data obtained from APOE*3-Leiden.CETP mice. *3: Repeated dosing. *4: As doses in diabetic patients are generally adapted to reach the desired plasma glucose level of < 8 mM, reductions are not depicted as percentages. Abbreviations: TC, total cholesterol; TG, triglycerides; GKA, glucokinase activator

References

1. Barengo NC, Katoh S, Moltchanov V, et al. The diabetes-cardiovascular risk paradox: results from a Finnish population-based prospective study. Eur Heart J. 2008 Aug;29(15):1889–95.
2. Sarwar N, Gao P, Seshasai SRK, et al. Diabetes mellitus, fasting blood glucose concentration, and risk of vascular disease: a collaborative meta-analysis of 102 prospective studies. Lancet (London, England). 2010 Jun;375(9733):2215–22.
3. Bae JC, Cho NH, Suh S, et al. Cardiovascular disease incidence, mortality and case fatality related to diabetes and metabolic syndrome: A community-based prospective study (Ansung-Ansan cohort 2001-12). J Diabetes. 2015 Nov;7(6):791–9.
4. Tarantino G, Saldalamacchia G, Conca P, et al. Non-alcoholic fatty liver disease: further expression of the metabolic syndrome. J Gastroenterol Hepatol. 2007 Mar;22(3):293–303.
5. Maric C, Hall JE. Obesity, metabolic syndrome and diabetic nephropathy. Contrib Nephrol. 2011;170:28–35.
6. Heinonen SE, Genove G, Bengtsson E, et al. Animal models of diabetic macrovascular complications: key players in the development of new therapeutic approaches. J Diabetes Res. 2015;2015:404085.
7. Lindstrom P. The physiology of obese-hyperglycemic mice [ob/ob mice]. ScientificWorldJournal. 2007 May;7:666–85.
8. Baker DJ, Atkinson AM, Wilkinson GP, et al. Characterization of the heterozygous glucokinase knockout mouse as a translational disease model for glucose control in type 2 diabetes. Br J Pharmacol. 2014 Apr;171(7):1629–41.
9. King AJF. The use of animal models in diabetes research. Br J Pharmacol. 2012 Jun;166(3):877–94.
10. Zadelaar S, Kleemann R, Verschuren L, et al. Mouse models for atherosclerosis and pharmaceutical modifiers. Arterioscler Thromb Vasc Biol. 2007 Aug;27(8):1706–21.
11. Ason B, van der Hoorn JWA, Chan J, et al. PCSK9 inhibition fails to alter hepatic LDLR, circulating cholesterol, and atherosclerosis in the absence of ApoE. J Lipid Res. 2014 Nov;55(11):2370–9.
12. van den Maagdenberg AM, Hofker MH, Krimpenfort PJ, et al. Transgenic mice carrying the apolipoprotein E3-Leiden gene exhibit hyperlipoproteinemia. J Biol Chem. 1993 May;;268(14):10540–5.
13. van Vlijmen BJ, van den Maagdenberg AM, Gijbels MJ, et al. Diet-induced hyperlipoproteinemia and atherosclerosis in apolipoprotein E3-Leiden transgenic mice. J Clin Invest. 1994 Apr;93(4):1403–10.
14. van de Steeg E, Kleemann R, Jansen HT, et al. Combined analysis of pharmacokinetic and efficacy data of preclinical studies with statins markedly improves translation of drug efficacy to human trials. J Pharmacol Exp Ther. 2013 Dec;347(3):635–44.
15. Delsing DJM, Jukema JW, van de Wiel MA, et al. Differential effects of amlodipine and atorvastatin treatment and their combination on atherosclerosis in ApoE*3-Leiden transgenic mice. J Cardiovasc Pharmacol. 2003 Jul;42(1):63–70.
16. Verschuren L, Kleemann R, Offerman EH, et al. Effect of low dose atorvastatin versus diet-induced cholesterol lowering on atherosclerotic lesion progression and inflammation in apolipoprotein E*3-Leiden transgenic mice. Arterioscler Thromb Vasc Biol. 2005 Jan;25(1):161–7.
17. van der Hoorn JWA, Kleemann R, Havekes LM, et al. Olmesartan and pravastatin additively reduce development of atherosclerosis in APOE*3Leiden transgenic mice. J Hypertens. 2007 Dec;25(12):2454–62.
18. van Vlijmen BJ, Pearce NJ, Bergo M, et al. Apolipoprotein E*3-Leiden transgenic mice as a test model for hypolipidaemic drugs. Arzneimittelforschung. 1998 Apr;48(4):396–402.
19. Delsing DJM, Post SM, Groenendijk M, et al. Rosuvastatin reduces plasma lipids by inhibiting VLDL production and enhancing hepatobiliary lipid excretion in ApoE*3-leiden mice. J Cardiovasc Pharmacol. 2005 Jan;45(1):53–60.
20. Kleemann R, Princen HMG, Emeis JJ, et al. Rosuvastatin reduces atherosclerosis development beyond and independent of its plasma cholesterol-lowering effect in APOE*3-Leiden transgenic mice: evidence for antiinflammatory effects of rosuvastatin. Circulation. 2003 Sep;108(11):1368–74.
21. Kooistra T, Verschuren L, de Vries-van der Weij J, et al. Fenofibrate reduces atherogenesis in ApoE*3Leiden mice: evidence for multiple antiatherogenic effects besides lowering plasma cholesterol. Arterioscler Thromb Vasc Biol. 2006 Oct;26(10):2322–30.
22. van der Hoorn JWA, de Haan W, Berbee JFP, et al. Niacin increases HDL by reducing hepatic expression and plasma levels of cholesteryl ester transfer protein in APOE*3Leiden.CETP mice. Arterioscler Thromb Vasc Biol. 2008 Nov;28(11):2016–22.

23. Postic C, Shiota M, Niswender KD, et al. Dual roles for glucokinase in glucose homeostasis as determined by liver and pancreatic beta cell-specific gene knock-outs using Cre recombinase. J Biol Chem. 1999 Jan;274(1):305–15.
24. Fajans SS, Bell GI, Bowden DW, et al. Maturity onset diabetes of the young (MODY). Diabet Med. 1996 Sep;13(9 Suppl 6):S90-5.
25. Velho G, Blanche H, Vaxillaire M, et al. Identification of 14 new glucokinase mutations and description of the clinical profile of 42 MODY-2 families. Diabetologia. 1997 Feb;40(2):217–24.
26. Gorman T, Hope DCD, Brownlie R, et al. Effect of high-fat diet on glucose homeostasis and gene expression in glucokinase knockout mice. Diabetes Obes Metab. 2008 Sep;10(10):885–97.
27. Baker DJ, Wilkinson GP, Atkinson AM, et al. Chronic glucokinase activator treatment at clinically translatable exposures gives durable glucose lowering in two animal models of type 2 diabetes. Br J Pharmacol. 2014 Apr;171(7):1642–54.
28. van Vlijmen BJ, van 't Hof HB, Mol MJ, et al. Modulation of very low density lipoprotein production and clearance contributes to age- and gender- dependent hyperlipoproteinemia in apolipoprotein E3-Leiden transgenic mice. J Clin Invest. 1996 Mar;97(5):1184–92.
29. Trion A, de Maat MPM, Jukema JW, et al. No effect of C-reactive protein on early atherosclerosis development in apolipoprotein E*3-leiden/human C-reactive protein transgenic mice. Arterioscler Thromb Vasc Biol. 2005 Aug;25(8):1635–40.
30. Post SM, Zoeteweij JP, Bos MH, et al. Acyl-coenzyme A:cholesterol acyltransferase inhibitor, avasimibe, stimulates bile acid synthesis and cholesterol 7alpha-hydroxylase in cultured rat hepatocytes and in vivo in the rat. Hepatology. 1999 Aug;30(2):491–500.
31. Kuhnast S, van der Tuin SJL, van der Hoorn JWA, et al. Anacetrapib reduces progression of atherosclerosis, mainly by reducing non-HDL-cholesterol, improves lesion stability and adds to the beneficial effects of atorvastatin. Eur Heart J. 2015 Jan;36(1):39–48.
32. Westerterp M, van der Hoogt CC, de Haan W, et al. Cholesteryl ester transfer protein decreases high-density lipoprotein and severely aggravates atherosclerosis in APOE*3-Leiden mice. Arterioscler Thromb Vasc Biol. 2006 Nov;26(11):2552–9.
33. Kuhnast S, van der Hoorn JWA, van den Hoek AM, et al. Aliskiren inhibits atherosclerosis development and improves plaque stability in APOE*3Leiden.CETP transgenic mice with or without treatment with atorvastatin. J Hypertens. 2012 Jan;30(1):107–16.
34. Stary HC, Chandler AB, Dinsmore RE, et al. A definition of advanced types of atherosclerotic lesions and a histological classification of atherosclerosis. A report from the Committee on Vascular Lesions of the Council on Arteriosclerosis, American Heart Association. Circulation. 1995 Sep;92(5):1355–74.
35. Kleiner DE, Brunt EM, Van Natta M, et al. Design and validation of a histological scoring system for nonalcoholic fatty liver disease. Hepatology. 2005 Jun;41(6):1313–21.
36. Liang W, Menke AL, Driessen A, et al. Establishment of a general NAFLD scoring system for rodent models and comparison to human liver pathology. PLoS One. 2014;9(12):e115922.
37. Tiniakos DG, Vos MB, Brunt EM. Nonalcoholic fatty liver disease: pathology and pathogenesis. Annu Rev Pathol. 2010;5:145–71.
38. Morrison MC, Mulder P, Salic K, et al. Intervention with a caspase-1 inhibitor reduces obesity-associated hyperinsulinemia, non-alcoholic steatohepatitis and hepatic fibrosis in LDLR-/-.Leiden mice. Int J Obes (Lond). 2016 Sep;40(9):1416–23.
39. Kotronen A, Yki-Jarvinen H, Mannisto S, et al. Non-alcoholic and alcoholic fatty liver disease - two diseases of affluence associated with the metabolic syndrome and type 2 diabetes: the FIN-D2D survey. BMC Public Health. 2010 May;10:237.
40. Lim H-W, Bernstein DE. Risk Factors for the Development of Nonalcoholic Fatty Liver Disease/Nonalcoholic Steatohepatitis, Including Genetics. Clin Liver Dis. 2018 Feb;22(1):39–57.
41. Di Angelantonio E, Sarwar N, Perry P, et al. Major lipids, apolipoproteins, and risk of vascular disease. JAMA. 2009 Nov;302(18):1993–2000.
42. Pettersson US, Walden TB, Carlsson P-O, et al. Female mice are protected against high-fat diet induced metabolic syndrome and increase the regulatory T cell population in adipose tissue. PLoS One. 2012;7(9):e46057.
43. Louet J-F, LeMay C, Mauvais-Jarvis F. Antidiabetic actions of estrogen: insight from human and genetic mouse models. Curr Atheroscler Rep. 2004 May;6(3):180–5.

44. Crespo CJ, Smit E, Snelling A, et al. Hormone replacement therapy and its relationship to lipid and glucose metabolism in diabetic and nondiabetic postmenopausal women: results from the Third National Health and Nutrition Examination Survey (NHANES III). Diabetes Care. 2002 Oct;25(10):1675–80.
45. Laakso M, Kuusisto J. Insulin resistance and hyperglycaemia in cardiovascular disease development. Nat Rev Endocrinol. 2014 May;10(5):293–302.
46. Roussel R, Steg PG, Mohammedi K,et al. Prevention of cardiovascular disease through reduction of glycaemic exposure in type 2 diabetes: A perspective on glucose-lowering interventions. Diabetes Obes Metab. 2018 Feb;20(2):238–44.
47. Liang W, Verschuren L, Mulder P, et al. Salsalate attenuates diet induced non-alcoholic steatohepatitis in mice by decreasing lipogenic and inflammatory processes. Br J Pharmacol. 2015 Nov;172(22):5293–305.
48. Zimmer M, Bista P, Benson EL, et al. CAT-2003: A novel sterol regulatory element-binding protein inhibitor that reduces steatohepatitis, plasma lipids, and atherosclerosis in apolipoprotein E*3-Leiden mice. Hepatol Commun. 2017 Jun;1(4):311–25.
49. Morrison MC, Liang W, Mulder P, et al. Mirtoselect, an anthocyanin-rich bilberry extract, attenuates non-alcoholic steatohepatitis and associated fibrosis in ApoE(*)3Leiden mice. J Hepatol. 2015 May;62(5):1180–6.
50. Ioannou GN, Haigh WG, Thorning D, et al. Hepatic cholesterol crystals and crown-like structures distinguish NASH from simple steatosis. J Lipid Res. 2013 May;54(5):1326–34.
51. Bakris GL, Williams M, Dworkin L, et al. Preserving renal function in adults with hypertension and diabetes: a consensus approach. National Kidney Foundation Hypertension and Diabetes Executive Committees Working Group. Am J Kidney Dis. 2000 Sep;36(3):646–61.
52. de Galan BE, Perkovic V, Ninomiya T, et al. Lowering blood pressure reduces renal events in type 2 diabetes. J Am Soc Nephrol. 2009 Apr;20(4):883–92.
53. Adingupu DD, Heinonen SE, Andreasson A-C, et al. Hyperglycemia Induced by Glucokinase Deficiency Accelerates Atherosclerosis Development and Impairs Lesion Regression in Combined Heterozygous Glucokinase and the Apolipoprotein E-Knockout Mice. J Diabetes Res. 2016;2016:8630961.
54. Princen HMG, Pouwer MG, Pieterman EJ. Comment on "Hypercholesterolemia with consumption of PFOA-laced Western diets is dependent on strain and sex of mice" by Rebholz S.L. et al. Toxicol. Rep. 2016 (3) 46-54. Toxicol reports. 2016;3:306–9.
55. Sattar N, Preiss D, Murray HM, et al. Statins and risk of incident diabetes: a collaborative meta-analysis of randomised statin trials. Lancet (London, England). 2010 Feb;375(9716):735–42.
56. Zinman B, Wanner C, Lachin JM, et al. Empagliflozin, Cardiovascular Outcomes, and Mortality in Type 2 Diabetes. N Engl J Med. 2015 Nov;373(22):2117–28.
57. Marso SP, Daniels GH, Brown-Frandsen K, et al. Liraglutide and Cardiovascular Outcomes in Type 2 Diabetes. N Engl J Med. 2016 Jul;375(4):311–22.
58. Marso SP, Bain SC, Consoli A, et al. Semaglutide and Cardiovascular Outcomes in Patients with Type 2 Diabetes. N Engl J Med. 2016 Nov;375(19):1834–44.